Macromolecules
ARTICLE

*Macromolecules* **2010**, *43*, 5925–5931 **5925**
DOI: 10.1021/ma101007x

# White Light-Emitting Devices Based on Star-Shape Polymers with a Bisindolylmaleimide Core

**Zhenghuan Lin,[†,‡] Yan-Duo Lin,[†] Cheng-Ya Wu,[‖] Po-Ting Chow,[§] Chia-Hsing Sun,[‖] and Tahsin J. Chow*[,†]**

[†]*Institute of Chemistry, Academia Sinica, Taipei 115, Taiwan,* [‡]*Department of Chemistry and Engineering, Huanghuai University, Zhumadian 463000, China,* [§]*Department of Chemistry, National Taiwan University, Taipei 106, Taiwan, and* [‖]*Department of Chemistry, Soochow University, Taipei 111, Taiwan*

*Received October 20, 2009; Revised Manuscript Received June 12, 2010*

ABSTRACT: A new type of star-shape polymers employing bisindolylmaleimide dye (**2a**−**c**) as the core and poly(2,7-fluorene) (PF) and/or poly(2,7-carbazole) (PC) as the arms were synthesized. These materials exhibited dual emissions consisting of an intensive blue luminescence from PF or PC and an orange emission from maleimide a result of partial energy transfer between the two. Highly efficient white light emitting devices were fabricated using a single emitting film made by spin-coating method. The electroluminescence (EL) properties of the devices were investigated from several directions, such as the loading amount of maleimide core, the concentration dependent spectral changes, the difference in the composition of arms, and the substituent effect in the indole segment, etc. A typical device based on the star-shape polymer **MF001** containing 0.01 mol % of core exhibited a maximal luminous efficiency of 7.2 cd/A and external quantum efficiency of 3.2%. The device based on **MMF001** with a methyl substituent on the indole group can be improved to reaching a maximal brightness of 11450 cd/m$^2$, and that based on **MFC1001** with arms comprising equal amount of PF and PC can be boosted to a maximal power efficiency of 4.8 lm/w. All devices can be fabricated readily and turned on at a considerable low voltage (< 5 V).

## Introduction

White light organic light-emitting diodes (WOLEDs) have attracted considerable attention in the past decade due to their potential applications in flat panel display and lighting applications.[1] With small molecules as emitters, WOLEDs have shown remarkable quantum efficiencies,[2] yet in practice, their applications have been severely hindered by the high cost of fabricating complicated multilayer devices. Devices employing a single emitting layer can be made by doping blue, green, and red dyes into a common host; in such a design it is crucial to control energy transfers among different dopants.[3] Recently, our group has employed hole transporting material (HTM) as a host containing 1% of a orange dopant to develop a simple WOLED device, ITO/dye (1%):NPB/TPBI/LiF/Al.[4] The white light intensity exceeded 10$^4$ cd/m$^2$; nevertheless, there still left plenty of room for further improvements.

Recently, white polymeric LEDs (WPLEDs) have demonstrated their great potential in future applications for their easy processing at low cost.[5] There are two major ways to get a white light emission from WPLEDs. The first is to blend red and blue polymer dyes together to form a single film.[6] However, these devices usually face the difficulties of low efficiency and/or color instability due to intrinsic phase separation. Another way is to prepare single polymer systems incorporating a red component into a blue polymer chain.[7] The optimal performance of these systems was comparable to those made with small molecules, and their high color stability has rendered them extremely promising in practical aspect.

Star-shape polymers have exhibited unusual properties for their highly branched and globular features capable of reducing intermolecular interactions. Wang and co-workers[8] have reported in a recent article that a star-shape polymer emitted white light with a notable luminous efficiency of 7.06 cd/A. In this report, we describe a new series of star-shape white electroluminescent polymers containing an orange core made of maleimide and three blue arms made of either polyfluorene or polycarbazole. Thin films made of these materials emit white light, which can be fabricated into WPLED with remarkable quantum efficiency.

## Experimental Section

**Materials.** Solvents were freshly distilled from appropriate drying agents prior to use. Commercial reagents were used without further purification unless otherwise stated. Precoated thin-layer chromatographic plates (TLC) and silica gel (230−400 mesh) were purchased from Merck. Compound **1a**−**c**,[9] **2a**−**b**,[4] **3**, and **4**[10] were synthesized according to reported procedures.

**Characterization.** Fast atom bombardment (FAB) mass spectra were recorded on a Jeol JMS 700 double-focusing spectrometer. Microanalyses were completed on a Perkin-Elmer 2400 elemental analyzer. NMR spectra were measured in $CDCl_3$ on a Bruker AVA300 FT-NMR spectrometer; $^1$H and $^{13}$C chemical shifts were quoted relative to the internal standard tetramethylsilane. UV−vis spectra were obtained on a HP-8453 spectrophotometer. The PL and EL properties were probed on a Hitachi F-4500 fluorescence spectrophotometer. The fluorescence quantum yields were determined in $CH_3CN$ solutions at 293 K against Nile red as a reference ($\Phi_p = 0.78$).[11] Cyclic voltammetry measurements were carried out on a BAS 100B electrochemical analyzer. A conventional three-electrode configuration consisting of a glassy carbon working electrode, a Pt-wire counter electrode and a $Ag/AgNO_3$ reference electrode was used. The supporting electrolyte was $[Bu_4N]PF_6$ (0.1 M). Ferrocene was added as an internal standard in each set of measurements, and all potentials were quoted with reference to the ferrocene−ferrocenium ($Fc/Fc^+$)

---

*Corresponding author. E-mail tjchow@chem.sinica.edu.tw.

couple at a scan rate of 100 mV·s$^{-1}$. The oxidation potential ($E_{\mathrm{ox}}$) was used to determine the HOMO energy level using the equation $E_{\mathrm{HOMO}} = -(E_{\mathrm{ox}} + 4.8)$ eV, which was calculated to the value of ferrocene (−4.8 eV).[12] Thermal analyses were performed with a Perkin-Elmer TGA6 thermal analyzer. Differential scanning calorimetry was done on a Perkin-Elmer DCS-7 instrument. The weight-average molecular weights ($M_{\mathrm{w}}$) and the polydispersity index (PDI) of soluble polymers were determined by gel-permeation chromatography (GPC) with a Waters 1515 instrument. The polystyrene and THF were used as standards and as eluent, respectively.

**Devices Fabrication.** Indium−tin oxide (ITO) with a sheet resistance of < 50 Ω was used as the substrate that was prepatterned by photolithography,[13] giving an effective device size of 4 mm$^2$. It was washed by detergent, deionized water and alcohol in sequence, followed by oxygen plasma cleaning. A 40 nm thick layer of poly(ethylenedioxythiophene):poly(styrenesulfonic acid) (PEDOT:PSS) was spin-coated onto the ITO glass substrate, followed by baking at 120 °C for 20 min. The polymer layer (70 nm) was then spin-coated on top of PEDOT:PSS layer, from a fresh toluene solution (10 mg/mL) through a Teflon filter (0.2 μm), and dried for 2 h at 90 °C under vacuum. An electron-transporting layer, 2,2′,2″-(1,3,5-benzeneriyl)tris(1-phenyl-1*H*-benzimidazole) (TPBI), was grown through thermal evaporation using ULVAC cryogenics at a chamber pressure of 10$^{-6}$ Torr. Finally, a thin layer of LiF (1 nm) was deposited onto the TPBI layer, followed by a layer of aluminum (120 nm).[14] The current−voltage and light-intensity measurements were done on a Keithley 2400 source meter and a Newport 1835C optical meter equipped with a Newport 818-ST silicon photodiode. All the fabrication and characterization of devices was carried out at ambient atmosphere.

**General Procedure of Core and A$_3$ Monomer Synthesis.** Compound **1** (1.00 mmol) was mixed with NaH (0.086 g, 3.6 mmol) in dried THF (7 mL) under a nitrogen atmosphere, and the solution turned gradually from red to dark blue. After the mixture was stirred with a magnetic bar for 15 min, benzylic bromide (3.6 mmol) was added to the mixture, while the solution began to turn red. The mixture was stirred for another 3 h at room temperature. The reaction was quenched by the addition of water (200 mL) and filtered. The filtrate was dissolved in dichloromethane and dried over MgSO$_4$. The crude product was purified by silica gel column chromatography with dichloromethane/hexane (1:3) as eluant to afford compound **2** as red solids.

*2,3-Bis(N-benzyl-2′-phenyl-3′-indolyl)-N-benzylmaleimide* (**2c**). Physical data of **2c** (yield 69%). $^1$H NMR (CDCl$_3$, 400 MHz): δ 4.72 (2H, s, Ar−CH$_2$), 5.00−5.14 (4H, m, 2 × Ar−CH$_2$), 6.58 (3H, br, Ar−H), 6.96 (5H, br, Ar−H), 7.02−7.15 (9H, m, Ar−H), 7.20 (4H, br, Ar−H), 7.26−7.28 (2H, m, Ar−H), 7.30 (2H, br, Ar−H), 7.31−7.33 (4H, m, Ar−H), 7.37 (4H, br, Ar−H). $^{13}$C NMR (CDCl$_3$, 100 MHz): δ 41.54, 47.77, 105.05, 110.52, 120.25, 120.87, 122.50, 125.94, 126.77, 127.17, 127.26, 127.44, 127.80, 128.22, 128.38, 128.61, 129.78, 131.54, 132.70, 137.12, 137.21, 137.43, 141.73, 170.49. HRMS (FAB): [M]$^+$ calcd, 749.3042; found, 749.3036.

*2,3-Bis(N-(4″-bromobenzyl)-3′-indolyl)-N-(4′-bromobenzyl)maleimide* (***2d***). Physical data of **2d** (yield 70%). $^1$H NMR (CDCl$_3$, 300 MHz): δ 4.77 (2H, s, Ar−CH$_2$), 5.24 (4H, s, 2 × Ar−CH$_2$), 6.72 (2H, t, *J* 7.3 Ar−H), 6.96 (6H, t, *J* 7.8, Ar−H), 7.04 (2H, t, *J* 7.6, Ar−H), 7.14 (2H, d, *J* 8.2 Ar−H), 7.32 −7.45 (8H, m, Ar−H), 7.67 (2H, s, Ar−H). $^{13}$C NMR (CDCl$_3$, 75 MHz): δ 41.20, 49.90, 106.51, 109.86, 120.31, 121.67, 121.79, 122.19, 122.60, 126.28, 127.06, 128.42, 130.35, 131.71, 131.75, 131.95, 135.48, 135.87, 136.16, 171.74. HRMS (FAB): [M]$^+$ calcd, 830.9732; found, 830.9739.

*2,3-Bis(N-(4″-bromobenzyl)-2′-methyl-3′-indolyl)-N-(4′-bromobenzyl)maleimide* (***2e***). Physical data of **2e** (yield 65%). $^1$H NMR (CDCl$_3$, 300 MHz): δ 1.98 (6H, br, Ar−CH$_3$), 4.82 (2H, s, Ar−CH$_2$), 5.12−5.18 (4H, m, 2 × Ar−CH$_2$), 6.55 (4H, br, Ar−H), 6.93 (2H, br, Ar−H), 7.10−7.21 (9H, m, Ar−H), 7.38−7.49 (5H, m, Ar−H). $^{13}$C NMR (CDCl$_3$, 75 MHz): δ 12.32, 41.38, 46.11, 104.73, 109.24, 120.31, 120.71, 121.27, 121.78, 122.06, 125.76, 127.46, 130.61, 131.82, 131.93, 135.78, 135.96, 136.79, 137.86, 171.11. HRMS (FAB): [M]$^+$ calcd, 859.0045; found, 859.0044.

*2,3-Bis(N-(4″-bromobenzyl)-2′-phenyl-3′-indolyl)-N-(4′-bromobenzyl)maleimide* (***2f***). Physical data of **2f** (yield 49%). $^1$H NMR (CDCl$_3$, 300 MHz): δ 4.58 (2H, s, Ar−CH$_2$), 4.91−5.03 (4H, m, 2 × Ar−CH$_2$), 6.46 (3H, br, Ar−H), 6.74 (4H, d, *J* 8.10, Ar−H), 7.01−7.07 (8H, m, Ar−H), 7.10 (2H, br, Ar−H), 7.17 (6H, br, Ar−H), 7.29−7.33 (4H, m, Ar−H), 7.35−7.39 (3H, m, Ar−H). $^{13}$C NMR (CDCl$_3$, 100 MHz): δ 40.96, 47.24, 105.11, 110.41, 120.89, 121.14, 121.40, 122.78, 126.71, 127.66, 127.91, 128.44, 129.67, 130.15, 131.33, 131.54, 131.80, 132.74, 136.01, 136.38, 137.03, 141.66, 170.24. HRMS (FAB): [M]$^+$ calcd, 983.0358; found, 983.0361.

**General Procedure for Suzuki Polymerization.** To a mixture of monomer **2**, **3**, and/or **4** under a nitrogen atmosphere was added Aliquat 336 (0.10 g, 0.25 mmol), aqueous K$_2$CO$_3$ (2 M, 2.5 mL), and toluene (6 mL). To it was added tetrakis(triphenylphosphine)-palladium (0.046 g, 0.04 mmol) while under nitrogen, and then the mixture was refluxed for 36 h. The polymerization was completed by refluxing with benzeneboronic acid (0.11 g, 1.0 mmol) for 6 h and with bromobenzene (0.10 mL, 1.0 mmol) for 8 h. The mixture was cooled to room temperature and poured into methanol. The precipitates were collected by filtration, dried, and then dissolved in dichloromethane. The solution was washed with water and dried over anhydrous MgSO$_4$. After most of the solvent being removed, the residue was poured into methanol with stirring to give polymer fiber. The polymer was further purified by extracting with acetone for 24 h using a Soxhlet apparatus. The final product was obtained after drying in vacuum with a yield of 40−55%.

*MF001*. Polymer **2d** (0.08 mg, 1 × 10$^{-4}$ mmol) and **3** (0.6 g, 1 mmol) were used in the polymerization. $^1$H NMR (300 MHz, CDCl$_3$): δ 0.82 (10H, br), 1.14 (20H, br), 2.13 (4H, br), 7.68 (4H, d, *J* 8.1), 7.83 (2H, d, *J* 10.5). GPC: $M_{\mathrm{w}}$ = 14500; PDI = 1.61.

*MF015*. Polymer **2d** (1.25 mg, 1.5 × 10$^{-3}$ mmol) and **3** (0.6 g, 1 mmol) were used in the polymerization. $^1$H NMR (300 MHz, CDCl$_3$): δ 0.82 (10H, br), 1.14 (20H, br), 2.12 (4H, br), 7.68 (4H, d, *J* 7.8), 7.83 (2H, d, *J* 9.9). GPC: $M_{\mathrm{w}}$ = 21300; PDI = 1.85.

*MF200*. Polymer **2d** (16.69 mg, 2 × 10$^{-2}$ mmol) and **3** (0.6 g, 1 mmol) were used in the polymerization. $^1$H NMR (300 MHz, CDCl$_3$): δ 0.82 (10H, br), 1.14 (20H, br), 2.11 (4H, br), 7.68 (4H, br), 7.83 (2H, br). GPC: $M_{\mathrm{w}}$ = 21400; PDI = 1.88.

*MMF001*. Polymer **2e** (0.09 mg, 1 × 10$^{-4}$ mmol) and **3** (0.6 g, 1 mmol) were used in the polymerization. $^1$H NMR (300 MHz, CDCl$_3$): δ 0.82 (10H, t), 1.14 (20H, br), 2.12 (4H, br), 7.68 (4H, d, *J* 8.5), 7.83 (2H, br). GPC: $M_{\mathrm{w}}$ = 19900; PDI = 1.79.

*PMF001*. Polymer **2f** (0.10 mg, 1 × 10$^{-4}$ mmol) and **3** (0.6 g, 1 mmol) were used in the polymerization. $^1$H NMR (300 MHz, CDCl$_3$): δ 0.82 (10H, t), 1.14 (20H, br), 2.12 (4H, br), 7.68 (4H, d, *J* 8.1), 7.83 (2H, d, *J* 10.8). GPC: $M_{\mathrm{w}}$ = 14500; PDI = 1.65.

*MFC1001*. Polymer **2d** (0.08 mg, 1 × 10$^{-4}$ mmol), **3** (0.3 g, 0.5 mmol) and **4** (0.3 g, 0.6 mmol) were used in the polymerization. $^1$H NMR (300 MHz, CDCl$_3$): δ 0.81−0.91 (33H, m), 1.04−1.13 (59H, m), 1.25−1.64 (27H, m), 2.12−2.24 (6H, m), 4.35 (4H, br), 7.37 −7.85 (29H, m), 8.17 (4H, br). GPC: $M_{\mathrm{w}}$ = 11600; PDI = 1.59.

*MFC2001*. Polymer **2d** (0.08 mg, 1 × 10$^{-4}$ mmol), **3** (0.2 g, 0.3 mmol) and **4** (0.4 g, 0.8 mmol) were used in the polymerization. $^1$H NMR (300 MHz, CDCl$_3$): δ 0.81−0.95 (17H, m), 1.02−1.40 (36H, m), 1.52−1.65 (25H, m), 2.15−2.27 (7H, m), 4.36 (4H, br), 7.49−7.88 (18H, m), 8.23 (5H, br). GPC: $M_{\mathrm{w}}$ = 12400; PDI = 1.41.

***MF001**, **MF015**, **MF200**, **MMF001**, and **PMF001***. All compounds showed similar NMR spectra. A typical spectrum of **MF001**: $^{13}$C NMR (CDCl$_3$, 75 MHz): δ 14.06, 22.59, 23.91, 29.22, 30.03, 31.79, 40.38, 55.33, 119.96, 121.48, 126.16, 127.19, 140.02, 140.49, 151.80. Polymers **MFC1001** and **MFC2001** showed similar NMR spectra. The spectrum of **MFC1001**: $^{13}$C NMR (CDCl$_3$, 75 MHz): δ 11.00, 14.03, 22.58, 23.11, 23.98, 24.50, 28.87, 29.23, 29.70, 30.09, 31.22, 31.77, 39.60, 40.46, 47.40, 55.34, 107.50, 107.96, 118.79, 119.19, 119.98, 120.55, 121.50, 121.97, Scheme 1

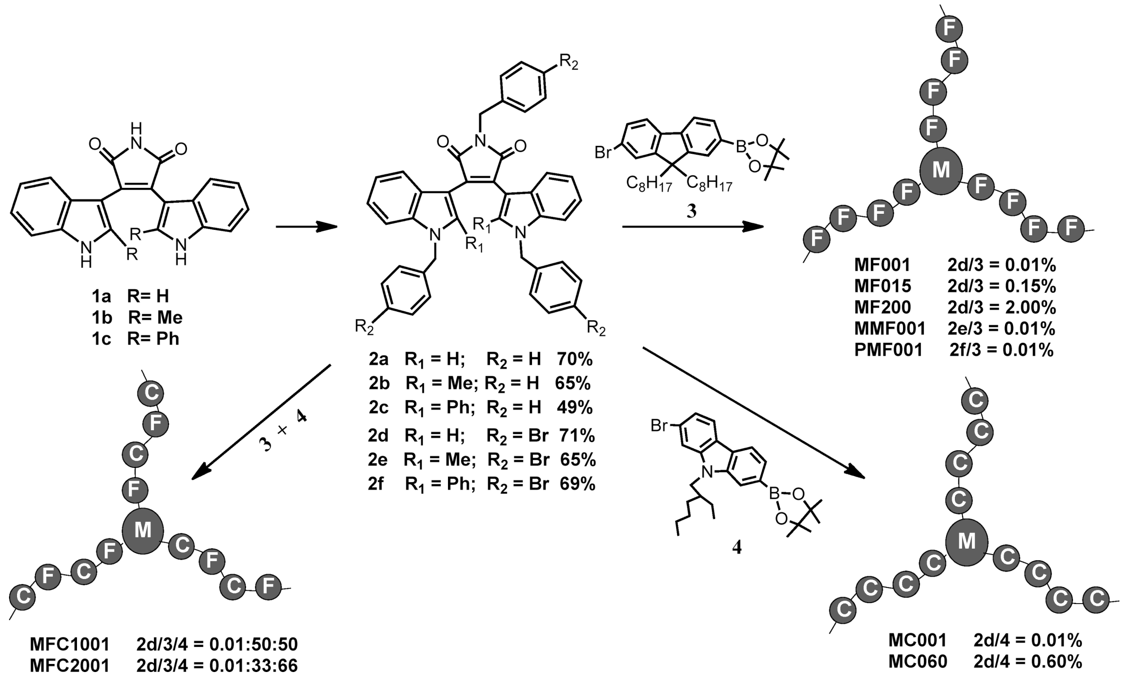

126.18, 126.46, 127.19, 128.39, 128.50, 128.76, 132.19, 139.57, 140.04, 140.18, 140.53, 141.10, 142.20, 151.82.

## Results and Discussion

**Synthesis of Monomers and Polymers.** The chemical structures and synthetic scheme of the designed polymers are shown in Scheme 1. The bisindolylmaleimide derivatives were chosen as the core because of their intensive red to orange colors.[9,15] Their long wavelength emissions are derived from charge transfer (CT) transitions, where the indole moieties act as electron donors and the maleimide carbonyl groups as electron acceptors. The presence of two cross-intercepting dipoles reduced the net polarity of molecules. Their round shape geometry along with flexible conformation reduced their tendency of crystallization, therefore resulted in high glass transition temperatures. Poly(2,7-fluorene) (PF) and poly(2,7-carbazole) (PC) are widely used as blue emitting dyes with large band gaps. They were selected as the arms of the star-shape polymers for their blue emission and outstanding electroluminescence (EL) efficiency.[16] Three kinds of polymers, i.e., **MF001**, **MC001**, and **MFC1001** were synthesized, where the capital letters denote maleimide (M), fluorene (F), and carbazole (C), respectively. The last three digits in **MF001** and **MC001** denote the content of the orange core in mol %. For **MFC1001**, the first number of the last four digits denotes a molar ratio of carbazole to fluorene.

The maleimides **2a−c** were synthesized readily through a substitution reactions with benzyl bromide from compounds **1a−c** with three kinds of substituents at C(2) of the indoles. In order to extend the chain lengths on the nitrogen substituents, a substituent need to be introduced at the para-position of the benzyl groups. The maleimide-based core units **2d−f** were synthesized in a similar manner with 4-bromobenzyl bromide in yields of 50−70%. Star-shape polymer were built up starting from the $A_3$ type units **2d−f**, which coupled with AB type monomers **3** or/and **4** by a one-pot Suzuki polycondensation reaction. By changing the feed ratios of M, F, and C units, a series of star-shape polymers were synthesized as listed in Scheme 1. All polymers are soluble in common organic solvents, such as toluene, chloroform and THF, except **MC001** and **MC060**. The chain length of arms might not be the same, as there was no control in the process of the polycondensation. In addition to the star-shaped polymers, there were unavoidably some detached arms coexisting in the media. The materials were used as obtained without further purification. The weight-average molecular weights ($M_w$) of these soluble polymers were estimated by gel permeation chromatography (GPC) using polystyrenes as internal standards, while the results revealed the range of 11600−21400 with polydispersity indexes (PDI) of 1.41−1.88.

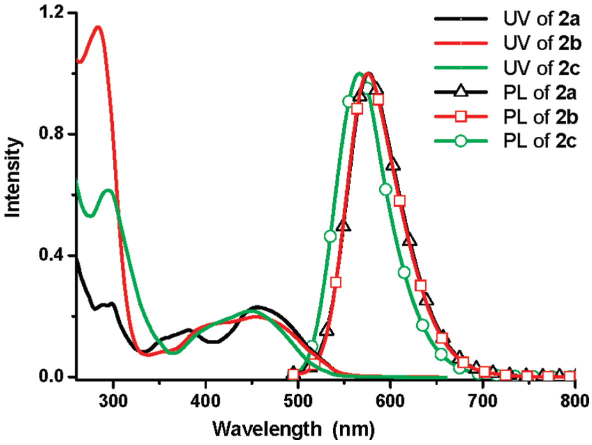

**Figure 1.** Absorption (left) and emission (right) spectra of compounds **2a−c** in dioxane. The excitation wavelength was 457 nm.

**Physical Properties of the Core.** The absorption spectra of maleimides **2a−c** in dioxane are shown in Figure 1. A high energy absorption band < 325 nm is known to derive from a $\pi-\pi^*$ transition localized mainly on the indole groups.[15b] The low energy absorption bands at > 325 nm can be assigned to the transitions involving both indole and maleimide moieties, because neither of them alone displays absorption at wavelength longer than 325 nm. The spectrum of **2a** displays two broad absorption bands at 381 and 459 nm.

The spectra of **2b** and **2c** are similar to each other, with a broad band at 463 and 450 nm, respectively, along with a shoulder at 406 and 400 nm. The difference of **2a** from **2b** and **2c** may be attributed to a more flexible conformation of the former through rotations along the C (maleimide)−C (indole) bond. Upon irradiation at 457 nm in dioxane, compounds **2a**−**c** yield intensive orange fluorescence at $\lambda_{max}$ 566−576 nm with quantum yields 0.32−0.61 (Table 1). It was well-recognized that these emissions come from charge transfer transitions, so that they exhibit apparent solvatochromic effect in different environments.[9]

Oxidation potentials were measured by cyclic voltammetry (CV) in THF with Ag/AgCl as a reference. The half-wave potentials of an oxidative sweep were measured to be 0.52, 0.62, and 0.51 eV for **2a**−**c**, respectively. The highest occupied molecular orbital (HOMO) levels were obtained by a comparison with the ionization potential of ferrocene at 4.8 eV (Table 1). The HOMO−LUMO (lowest unoccupied molecular orbital) band gaps were estimated at the interception wavelength of absorption and emission spectra, and were found to be 2.33 (**2a**), 2.35 (**2b**) and 2.37 (**2c**) eV. The absorption spectra of **2a**−**c** overlapped with the emission spectra of fluorene and carbazole (ESI S1), thus assured a feasible energy transfer. From the energy level diagram it was also found that the positions of HOMO and LUMO energy levels of **2a**−**c** lay within the corresponding band region of either fluorene or carbazole. Therefore, energy transfer from the outer arms of the star-shape polymer to the central core is energetically favorable. By controlling the loading amounts of **2d**−**f** with respect to the fluorene or carbazole units, polymers suitable for producing white emission can be prepared plausibly.

**Physical Properties of the Polymers.** By changing the molar ratio of the core **2a**, three kinds of star-shape polymers **MF001**, **MF015**, and **MF200** were synthesized. Their absorption spectra exhibited a strong absorption band at ca. 384 nm in toluene as well as in the solid state, which derives mainly from the fluorene segments (ESI S2).[16a] The absorption band deriving from the maleimide core cannot be distinguished due to its low content. The luminescence spectra of polymers **MF001** and **MF015** in toluene exhibited dominant blue emissions at ca. 420 nm deriving from PF, except **MF200** which showed a minor shoulder at 570 nm (Figure 2). The emission spectra in the solid state displayed a distinctly different appearance. In films the relative intensity of the yellow emissions at 540−555 nm became much more pronounced comparing to the blue bands at ca. 430 nm. The blue component diminished nearly to nil when the ratio of M reached a level of 2%, i.e., in the case of **MF200** (Figure 2). It is evident that intermolecular energy transfer plays a major role in the solid state as a result of closer stacking of molecules. A substantial red shift of the yellow bands was also observed along with the increase of the M ratio. It can be explained by a gradual increase of the polarity of the media, because the polarity of maleimide is substantially higher than that of fluorene. The influence of substituent was also explored by examining the emission spectra of polymers **MMF001** and **PMF001**, in which a methyl or a phenyl group was added onto the indole moieties of maleimide (Scheme 1). In their PL spectra, they all exhibit dual emissions at both 445 and 537 nm, indicating a negligible effect of substituent groups on the indoles (ESI S3).

**Table 1. Physical Data of Compounds 2a−c**[a]

| compound | absorption (nm) | emission (nm) | $\Phi_p$ | HOMO (eV) | LOMO (eV) |
|---|---|---|---|---|---|
| **2a** | 298, 381, 459 | 576 | 0.42 | 5.32 | 2.99 |
| **2b** | 284, 463 | 575 | 0.32 | 5.42 | 3.07 |
| **2c** | 295, 450 | 566 | 0.61 | 5.31 | 2.94 |

[a] Spectra taken in dioxane, excitation wavelength 457 nm.

The energy transfer characteristics of the polymers were further examined at different concentrations. As mentioned above, these materials were composed of both the star-shape polymers and also some detached polyfluorene arms. In highly diluted solutions, ET was confined as an intramolecular process, while each unit of **MF200** emits a red light in the solution and each detached polyfluorene arm emits a blue light. The combined emission was a broad band spectrum with double maxima. The relative intensities between the red and the blue bands maintained a constant independent to concentration (Figure 3a). When the concentration increased, e.g., over 0.01 mg/mL (ca. $10^{-6}$ M) in toluene, intermolecular processes started to appear. The intensity of red band increased at the expenses of the blue band. The trend can be clearly depicted by the normalized spectra given in Figure 3a. The lowest red/blue ratio at high dilution was determined by the relative amount of detached polyfluorene arms. For the purpose of comparison, a reference mixture was prepared by blending **2a** into pure polyfluorene with the same ratio as that preparing **MF200**. At high concentration this mixture displayed a similar behavior as that of **MF200**. However, at low concentration the red emission diminished to nil as a result of lacking of intramolecular ET, which was feasible only in star-shape polymers (Figure 3b).

The polarity of carbazole is higher than fluorene; therefore, it was anticipated that replacing the PF side arms by PC may induce a red shift on the emission of the M core.[4,17] A slight red shift is helpful for adjusting the emission spectrum

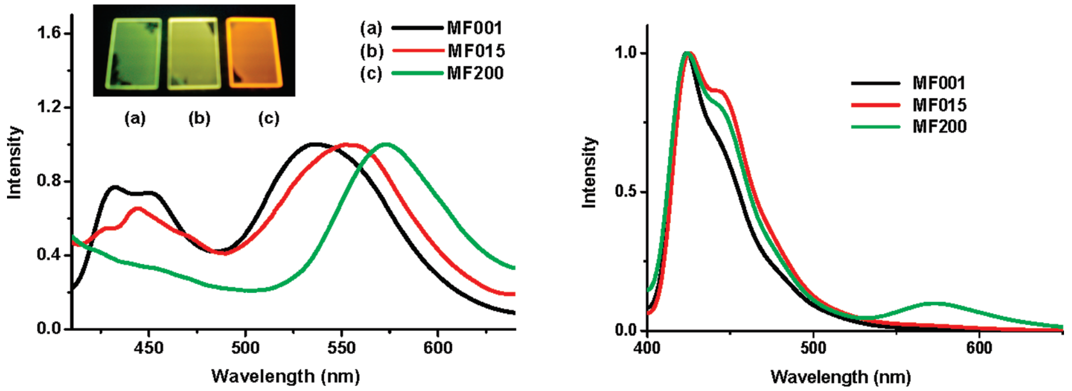

**Figure 2.** Emission spectra of polymers **MF001**, **MF015**, and **MF200** in solid film (left) and toluene (right, at 0.01 mg/mL) upon excitation at 380 nm. The photographs in the inset correspond to the spectra with different core concentrations.

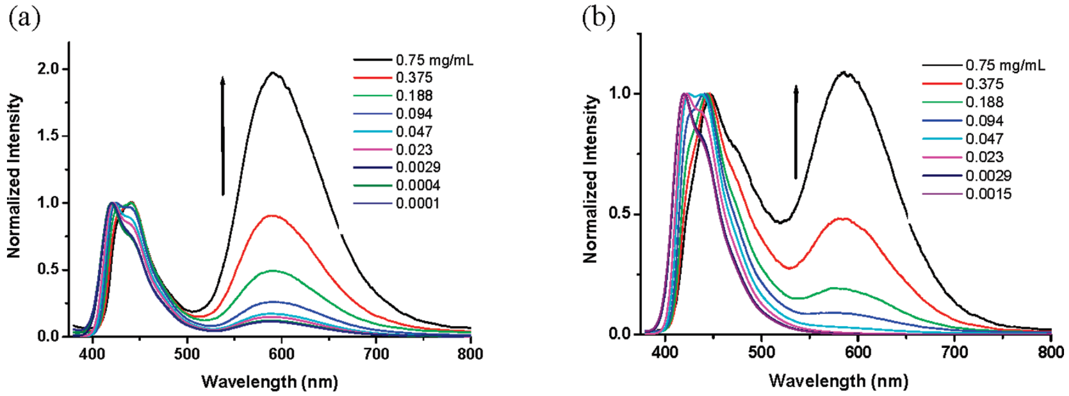

**Figure 3.** (a) Concentration dependent emission spectra of **MF200** in toluene excited at 380 nm. The intensity of red component increases along with the increase of concentration, as a result of intermolecular energy transfer. The ratio of red/blue stays invariant at high dilution while energy transfer processes are limited within each molecular strand. (b) Emission spectra of a material prepared by blending **2a** into polyfluorene with the same core/arm ratio as **MF200**. It displays a similar concentration dependent behavior at high concentration. At low concentration the red band diminished as a consequence of lacking of significant intramolecular energy transfer. All the spectra in parts a and b were normalized at the blue emission band for easy comparison.

toward a standard white light. Polymers with PC side arms, e. g. **MC001** and **MC060**, were synthesized in this regard. Comparing to the spectrum of **MF001**, their long wavelength emissions appeared at ca. 583 nm, which did exhibit a considerable red shift with respect to the PF polymers (ESI S4). However, the solubility of PC polymers was considerably lower than those of the PF polymers. For example, the solubility of **MC001** and **MC060** was so low that it was difficult to make workable film through solution processes. To overcome the solubility problem, copolymer **MFC1001** and **MFC2001** were prepared by mixing fluorene with carbozole together. According to the relative integrations in the $^1$H NMR spectra of **MFC1001** and **MFC2001**, the actual ratios of C to F in polymer arms were estimated to be 0.65 and 1.25, respectively (ESI S5). These polymers did express better solubility in most organic solvents. In their emission spectra (Figure 4), the red bands deriving from maleimide appeared at 546 and 552 nm, which did exhibited a ca. 20 nm red shift comparing to that of **MF001**.

The thermal properties of these star-shape polymers were investigated by thermogravimetric analysis (TGA) and differential scanning calorimetry (DSC) under a nitrogen atmosphere. All polymers showed high thermal stability. According to the TGA plot of **MF001**, only a slight weight loss (< 5%) can be detected before 423 °C (ESI S6), and only at a higher temperature the polymer chain started to collapse. A glass transition temperature ($T_g$) of **MF001** was detected at 112 °C as shown in a DSC sweep (Figure S6 inset). The relatively high values of $T_g$ and $T_d$ (thermal decomposition temperature) help to suppress morphological changes during the operation of devices.

**White Electroluminescence from Single Films.** To investigate the EL characteristics of these star-shape polymers, devices were fabricated with the configuration of ITO/PEDOT:PSS (40 nm)/polymer (70 nm)/TPBI (30 nm)/LiF (1 nm)/Al (120 nm). In this device, PEDOT:PSS was employed as a hole-injecting material and TPBI as an electronic-transporter as well as hole-blocker. All polymers exhibited dual emissions, whereas the relative intensities between the two depends on the relative amount of maleimide core. The EL spectra derived from the devices made with **MF001**, **MF015**, and **MF200** are compared in Figure 5. The spectrum of **MF001** displayed a broad band with fwhm (full width at half-maximum) ca. 155 nm ranging from 415 to 570 nm. Its CIE coordinate at (0.23, 0.33) was a little away from standard white light (0.33, 0.33) due to the blue shift of maleimide emission in a nonpolar environment. Increasing the content of maleimide in the polymers from 0.01% mol (**MF001**) to 0.15% (**MF015**) and 2% mol (**MF200**), the red component was shifted successfully to 539 and 561 nm. The CIE coordinates at (0.30, 0.40) and (0.36, 0.40) moved closer to the standard white light. However, the increase of loading amount of the M core resulted to a

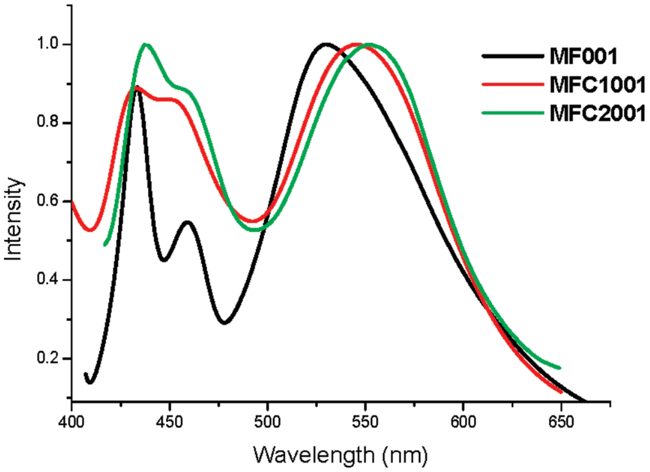

**Figure 4.** Emission spectra of polymers **MF001**, **MFC1001**, and **MFC2001** in solid film.

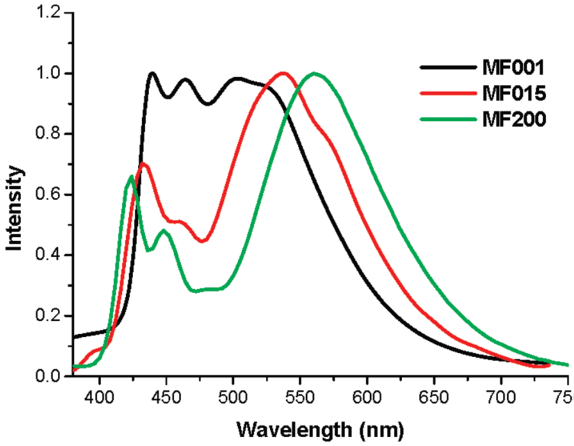

**Figure 5.** Electroluminescence spectra of polymers **MF001**, **MF015** and **MF200** in WPLEDs.

**Table 2. Performance of Devices Made with Star-Like Polymers**

| polymer | turn on (v) | maximum brightness (cd/m$^2$) | maximum luminous efficiency (cd/A) | maximum power efficiency (lm/W) | maximum quantum efficiency (%) | CIE ($x$, $y$) |
|---|---|---|---|---|---|---|
| MF001 | 5.0 | 7728 | 7.20 | 3.48 | 3.21 | (0.23, 0.33) |
| MF015 | 5.3 | 4962 | 4.16 | 2.38 | 1.89 | (0.30, 0.40) |
| MF200 | 5.7 | 3960 | 3.95 | 2.07 | 1.52 | (0.36, 0.40) |
| MMF001 | 4.5 | 11450 | 6.69 | 4.09 | 2.62 | (0.28, 0.37) |
| PMF001 | 4.5 | 1190 | 2.93 | 1.68 | 1.10 | (0.28, 0.39) |
| MFC1001 | 4.0 | 8994 | 6.09 | 4.78 | 2.42 | (0.26, 0.36) |
| MFC2001 | 4.0 | 6483 | 4.61 | 3.22 | 1.85 | (0.29, 0.36) |

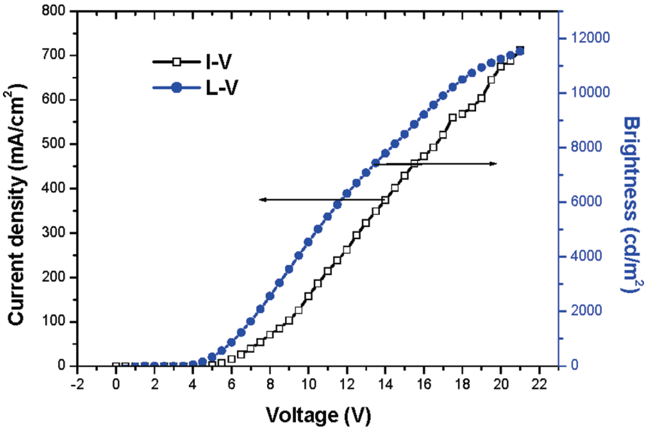

**Figure 6.** Plots of current density I (□) and brightness L (●) versus voltage $V$ of device made with **MMF001**.

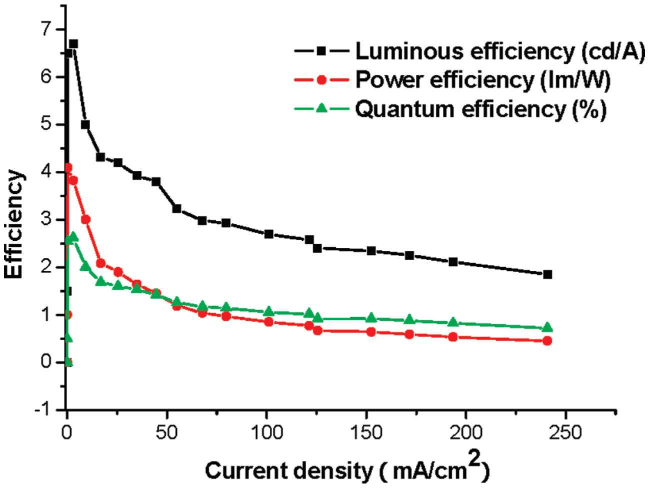

**Figure 7.** Plots of luminance efficiency, power efficiency, and external quantum efficiency versus current density of device made with **MMF001**.

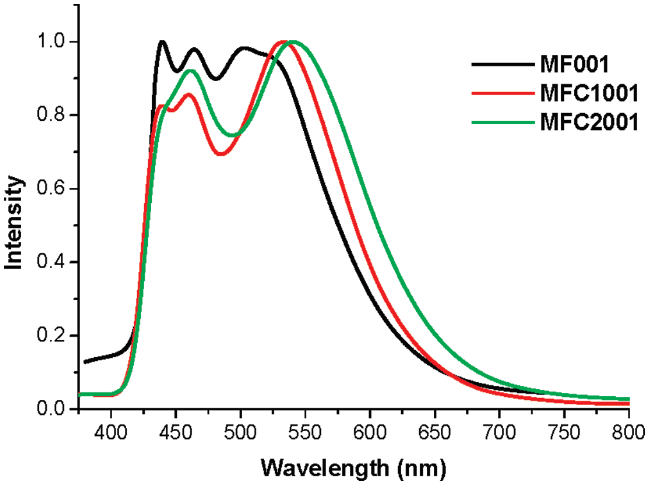

**Figure 8.** Electroluminescence spectra of polymers **MF001**, **MFC1001** and **MFC2001** in WPLEDs.

decrease of EL efficiency along with an increase of turn-on voltages (Table 2). The device made with **MF001** performed the best, i.e., with luminance, power and quantum efficiencies of 7.20 cd/A, 3.48 lm/W, and 3.21%, respectively. The maximal brightness reached to 7728 cd/m$^2$. When the content of M was increased to 2% mol, maximum brightness and efficiencies reduced to almost half those of **MF001**. Such differences may be ascribed to a concentration quenching of maleimides, along with possible charge-trapping effect.[8,18]

The substituent effect of maleimide core was investigated in the next stage by changing the substituent on the indole groups.[9] Polymers **MMF001** and **PMF001** were synthesized with methyl and phenyl substituents attached onto the C(2′) position of the indoles in M. With increased bulkiness of the group, the relative intensity of the maleimide emission became higher (ESI S7). It seems that the energy transfer from polyfluorene to maleimide increased in the order of **PMF001** > **MMF001** > **MF001**. A slight red shift was also observed on the long wavelength band, although the amount of shift may not sufficient enough for composing a pure white light. The device made with **MMF001** displayed an emission with a CIE coordinate of (0.28, 0.37), which is getting closer to a white light than that of (0.23, 0.33) made with **MF001**. Their EL properties are shown in Table 2. The device made from **MMF001** displayed a maximum luminance efficiency 6.69 cd/A, power efficiency 4.09 lm/W and quantum efficiency 2.62% with turn-on voltage 4.5 V. Moreover, their broad band EL spectra were quite stable in a voltage range of 6−15 V (ESI S8). According to the $I-V-L$ plots in Figure 6, the brightness can reach to 11450 cd/m$^2$ at 21 V with a low turn-on voltage 4.5 V. Plots of device performance versus current density are given in Figure 7. The luminance, power and quantum efficiency decreased only mildly with an increasing of current density.

Carbazole is known to be a blue emitter with good hole transporting ability, while its molecular structure is more polar than fluorene. Replacing the fluorene units in polymer chains with carbazole units was able to increase the polarity of the polymer films. In their emission spectra of copolymers **MFC1001** and **MFC2001**, the maleimide band indeed showed a red shift comparing to that of **MF001**. The devices made with **MFC1001** and **MFC2001** by spin coating method displayed broad band emissions with CIE coordinates at (0.26, 0.36) and (0.29, 0.36) (Figure 8). Their performances are compatible with those made with **MF001** (Table 2), e.g. with similar brightness, lower turn-on voltage, yet slightly lower quantum efficiency. The maximum brightness, luminance, power and quantum efficiencies of **MFC1001** were measured to be 8994 cd/m$^2$, 6.90 cd/A, 4.78 lm/W, and 2.42%, respectively, along with a turn-on voltage at 4.0 V. Their EL spectra was stable with respect to the applied bias in the range of 6−10 V (ESI S9). The plots of inter-relationships among voltage, current density, brightness, and efficiency of the device made with **MFC1001** can be found in the Supporting Information (ESI S10, S11). According to such a performance, it is apparent that inserting carbazole units into the arms of star-shape polymers is a promising way to improve their EL properties toward the design of white light devices. Further improvements can be expected along this direction.

## Conclusions

In summary, we have developed an efficient way of preparing star-shape polymers using bisindolylmaleimide as the core for producing white light LEDs. These materials exhibit blue emission from polyfluorene and yellow to red emission from the maleimide. The spectra of devices can be adjusted by changing the molar ratio of maleimide to fluorene. The range of a ratio in 0.01−2% has been examined, while the electroluminescence displayed dual bands covering the wavelength region of 400−700 nm. In highly diluted solutions, the materials displayed a bluish color due to the low content of maleimide, yet in condensed phases such as solid films the materials emit white light as a result of significant intermolecular energy transfer. To further adjust the wavelength toward standard white light, carbazole can be added into the polymer chains to red shift the long wavelength componentn. The devices made with them performed remarkable well, and in CIE coordinate the color approached reasonably close to the standard white light. The materials made by blending carbazole and fluorene together has the advantages of high solubility for easy processing, ready accessibility and fabrication, good thermal stability and reliable color under wide operating voltages, etc. These star-shape polymers have revealed promising results for producing white light from a single film of polymers.

**Acknowledgment.** This work was supported by Academia Sinica and the National Science Council of the Republic of China.

**Supporting Information Available:** Figures showing absorption spectra of polymer **MF001**, **MF015**, and **MF200** both in solutions and in solid films, emission spectra of **PF** and **PC** in $CH_2Cl_2$, emission spectra of polymers **MF001**, **MMF001**, **PMF001**, **MC001**, and **MC060** in solid films, $^1$H NMR spectra of **MFC1001** and **MFC2001**, TGA and DSC plots of **MF001**, HOMO and LUMO energy levels of **2a−c**, **PF** and **PC**, electroluminescence of polymers **MF001**, **MMF001**, **PMF001**, and **MFC1001**, and plots of device parameters made with **MFC1001**. This material is available free of charge via the Internet at http://pubs.acs.org.

## References and Notes

(1) (a) Paik, K. L.; Baek, N. S.; Kim, H. K.; Lee, J.-H.; Lee, H. *Macromolecules* **2002**, *35*, 6782. (b) D'Andrade, B. W.; Forrest, S. R. *Adv. Mater.* **2004**, *16*, 1585. (c) Liu, Y.; Nishiura, M.; Wang, Y.; Hou, Z. M. *J. Am. Chem. Soc.* **2006**, *128*, 5592. (d) Coppo, P.; Duati, M.; Kozhevnikov, V. N.; Hofstraat, J. W.; De Cola, L. *Angew. Chem., Int. Ed.* **2005**, *44*, 1806. (e) Furuta, P. T.; Deng, L.; Garon, S.; Thompson, M. E.; Fréchet, J. M. *J. Am. Chem. Soc.* **2003**, *125*, 13165. (f) Niu, X.; Ma, L.; Yao, B.; Ding, J.; Tu, G.; Xie, Z.; Wang, L. *Appl. Phys. Lett.* **2006**, *89*, 213508. (g) Holmes, R. J.; Forrest, S. R.; Tung, Y. J.; Kwong, R. C.; Brown, J. J.; Garon, S.; Thompson, E. M. *App. Phys. Lett.* **2003**, *82*, 2422.

(2) (a) Shao, Y.; Yang, Y. *Appl. Phys. Lett.* **2005**, *86*, 073510. (b) D'Andrade, B. W.; Thompson, M. E.; Forrest, S. R. *Adv. Mater.* **2002**, *14*, 147. (c) Kido, J.; Kimura, M.; Nagai, K. *Science* **1995**, *267*, 1332. (d) Ho, C.-L.; Wong, W.-Y.; Wang, Q.; Ma, D.; Wang, L.; Lin, Z. *Adv. Funct. Mater.* **2008**, *18*, 928. (e) Jiang, C.; Yang, W.; Peng, J.; Xiao, S.; Cao, Y. *Adv. Mater.* **2004**, *16*, 537.

(3) (a) D'Andrade, B. W.; Holmes, R. J.; Forest, S. R. *Adv. Mater.* **2004**, *16*, 624. (b) Holmes, R. J.; D'Andrade, B. W.; Ren, X.; Li, J.; Thompson, M. E.; Forrest, S. R. *Appl. Phys. Lett.* **2003**, *83*, 3818. (c) Sun, Y.; Giebink, N. C.; Kanno, H.; Ma, B.; Thompson, M. E.; Forrest, S. R. *Nature* **2006**, *440*, 908.

(4) Lin, Z.; Wen, Y.-S.; Chow, T. J. *J. Mater. Chem.* **2009**, *19*, 5141.

(5) Raja, I. ul H.; Lee, J. Y.; Kim, In T.; Lee, S. H. *Monatsh. Chem.* **2008**, *139*, 725.

(6) (a) Tokio, S.; Suzuki, M.; Sato, F.; Kamachi, M.; Shirane, K. *Org. Electron.* **2003**, *4*, 105. (b) Shih, P. I.; Tseng, Y. H.; Wu, F. I.; Dixit, A. K.; Shu, C. F. *Adv. Funct. Mater.* **2006**, *16*, 1582. (c) Su, H. J.; Wu, F. I.; Shu, C. F. *Macromolecules* **2004**, *37*, 7197. (d) Hwang, D. H.; Park, M. J.; Kim, S. K.; Lee, N. H.; Kim, Y. B.; Shim, H. K. *J. Mater. Res.* **2004**, *19*, 2081.

(7) (a) Tsai, M.-L.; Liu, C.-Y.; Hsu, M.-A.; Chow, T. J. *Appl. Phys. Lett.* **2003**, *82*, 550. (b) Chuang, C.-Y.; Shih, P.-I.; Chien, C.-H.; Wu, F.-I.; Shu, C.-F. *Macromolecules* **2007**, *40*, 247. (c) Lee, S. K.; Hwang, D. H.; Jung, B. J.; Cho, N. S.; Lee, J.; Lee, J. D.; Shim, H. K. *Adv. Funct. Mater.* **2005**, *15*, 1647. (d) Wu, W. C.; Lee, W. Y.; Chen, W. C. *Macromol. Chem. Phys.* **2006**, *207*, 1131. (e) Furua, P. T.; Deng, L.; Garon, S.; Thompson, M. E.; Fréchet, J. M. J. *J. Am. Chem. Soc.* **2004**, *126*, 15388. (f) Kawamoto, M.; Tsukamoto, T.; Kinoshita, M.; Ikeda, T. *Appl. Phys. Lett.* **2006**, *89*, 121920. (g) Zhen, H.; Xu, W.; Yang, W.; Chen, Q.; Xu, Y.; Jiang, J.; Peng, J.; Cao, Y. *Macromol. Rapid Commum.* **2006**, *27*, 2095.

(8) Liu, J.; Cheng, Y.; Xie, Z.; Geng, Y.; Wang, L.; Jing, X.; Wang, F. *Adv. Mater.* **2008**, *20*, 1357.

(9) (a) Chiu, C. W.; Chow, T. J.; Chuen, C. H.; Lin, H. M.; Tao, Y. T. *Chem. Mater.* **2003**, *15*, 4527. (b) Yeh, T. S.; Chow, T. J.; Tsai, S. H.; Chiu, C. W.; Zhao, C. X. *Chem. Mater.* **2006**, *18*, 832.

(10) (a) Sandee, A. J.; Williams, C. K.; Evans, N. R.; Davies, J. E.; Boothby, C. E.; Köhler, A.; Friend, R. H.; Holmes, A. B. *J. Am. Chem. Soc.* **2004**, *126*, 7041. (b) Dierschke, F.; Grimsdale, A. C.; Müllen, K. *Synthesis* **2003**, *16*, 2470.

(11) Sarkar, N.; Das, K.; Nath, D. N.; Bhattacharyya, K. *Langmuir* **1994**, *10*, 326.

(12) (a) Pommerehne, J.; Vestweber, H.; Guss, W.; Mahrt, R. F.; Bässler, H.; Porsch, M.; Daub, J. *Adv. Mater.* **1995**, *7*, 551. (b) Thelakkat, M.; Schmidt, H. W. *Adv. Mater.* **1998**, *10*, 219.

(13) Menard, E.; Meitl, M. A.; Sun, Y.; Park, J.-U.; Shir, D. J.-L.; Nam, Y.-S.; Jeon, S.; Rogers, J. A. *Chem. Rev.* **2007**, *107*, 1117.

(14) Hung, L. S.; Tang, C. W.; Mason, M. G. *Appl. Phys. Lett.* **1997**, *70*, 152.

(15) (a) Chan, L. H.; Lee, Y. D.; Chen, C. T. *Macromolecules* **2006**, *39*, 3262. (b) Kaletas, B. K.; Mandl, C.; Zwan, G.; Fanti, M.; Zerbeto, F.; Cola, L. D.; Konig, B.; Williams, R. M. *J. Phys. Chem. A* **2005**, *109*, 6440. (c) Wu, W. C.; Yeh, H. C.; Chan, L. H.; Chen, C. T. *Adv. Mater.* **2002**, *14*, 1072. (d) Chow, T. J.; Tsai, S. H.; Chiu, C. W.; Yeh, T. S. *Synth. Met.* **2005**, *149*, 59.

(16) (a) Scherf, U.; List, E. J. W. *Adv. Mater.* **2002**, *14*, 477. (b) Michinobu, T.; Kumazawa, H.; Otsuki, E.; Usui, H.; Shigehara, K. *J. Polym. Sci., Part A: Polym. Chem.* **2009**, *47*, 3880.

(17) Liu, J.; Zhou, Q.; Cheng, Y.; Geng, Y.; Wang, L.; Ma, D.; Jing, X.; Wang, F. *Adv. Funct. Mater.* **2006**, *16*, 957.

(18) (a) Liu, J.; Tu, G. L.; Zhou, Q. G.; Cheng, Y. X.; Geng, Y. H.; Wang, L. X.; Ma, D. G.; Jing, X. B.; Wang, F. S. *J. Mater. Chem.* **2006**, *16*, 1431. (b) Shaheen, S. E.; Lippelen, B.; Peyghambarian, N.; Wang, J.-F.; Anderson, J. D.; Mash, E. A.; Lee, P. A.; Armstrong, N. R.; Kawabe, Y. *J. Appl. Phys.* **1999**, *85*, 7939.